

Accepted Manuscript

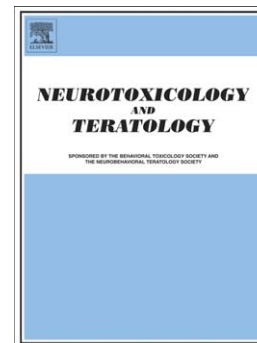
Structural brain abnormalities in patients with inflammatory illness acquired following exposure to water-damaged buildings: A volumetric MRI study using NeuroQuant®

Ritchie C. Shoemaker, Dennis House, James C. Ryan

PII: S0892-0362(14)00132-9
DOI: doi: [10.1016/j.ntt.2014.06.004](https://doi.org/10.1016/j.ntt.2014.06.004)
Reference: NTT 6469

To appear in: *Neurotoxicology and Teratology*

Received date: 7 October 2013
Revised date: 3 June 2014
Accepted date: 5 June 2014



Please cite this article as: Ritchie C. Shoemaker, Dennis House, James C. Ryan, Structural brain abnormalities in patients with inflammatory illness acquired following exposure to water-damaged buildings: A volumetric MRI study using NeuroQuant®, *Neurotoxicology and Teratology* (2014), doi: [10.1016/j.ntt.2014.06.004](https://doi.org/10.1016/j.ntt.2014.06.004)

This is a PDF file of an unedited manuscript that has been accepted for publication. As a service to our customers we are providing this early version of the manuscript. The manuscript will undergo copyediting, typesetting, and review of the resulting proof before it is published in its final form. Please note that during the production process errors may be discovered which could affect the content, and all legal disclaimers that apply to the journal pertain.

Structural brain abnormalities in patients with inflammatory illness acquired following exposure to water-damaged buildings: a volumetric MRI study using NeuroQuant®

Ritchie C. Shoemaker MD¹, Dennis House¹ and James C. Ryan²,
¹Center for Research on Biotoxin Associated Illnesses, Pocomoke, Md
² Proteogenomics, Vero Beach, Florida

Corresponding author: Ritchie C. Shoemaker, MD 500 Market St Suite 103 Pocomoke, Md 21851. ritchieshoemaker@msn.com.

Key words: NeuroQuant, caudate nucleus, microscopic interstitial edema, blood brain barrier, inflammation, TGF-B1 beta, VEGF, MMP9, volumetric MRI, neuropsychiatry

Abbreviations used:

BBB blood brain barrier
C4a split product of activation of complement component 4
CIRS-WDB chronic inflammatory response syndrome caused by exposure to the interior environment of water-damaged buildings
CN caudate nucleus
CNS central nervous system
ERMI Environmental Relative Moldiness Index
GFAP glial fibrillary acidic protein
MMP9 matrix metalloproteinase 9
MRI magnetic resonance imaging
MRS magnetic resonance spectroscopy
NQ NeuroQuant
TGFB1 transforming growth factor beta-1
TS Tourette's Syndrome
VEGF vascular endothelial growth factor
VIP vasoactive intestinal polypeptide

Abstract

Executive cognitive and neurologic abnormalities are commonly seen in patients with a chronic inflammatory response syndrome (CIRS) acquired following exposure to the interior environment of water-damaged buildings (WDB), but a clear delineation of the physiologic or structural basis for these abnormalities has not been defined. Symptoms of affected patients routinely include headache, difficulty with recent memory, concentration, word finding, numbness, tingling, metallic taste and vertigo. Additionally, persistent proteomic abnormalities in inflammatory parameters that can alter permeability of the blood brain barrier, such as C4a, TGFB1, MMP9 and VEGF, are notably present in cases of CIRS-WDB compared to controls, suggesting consequent inflammatory injury to the central nervous system. Findings of gliotic areas in MRI scans in over 45% of CIRS-WDB cases compared to 5% of controls, as well as elevated lactate and depressed ratios of glutamate to glutamine are regularly seen in MR spectroscopy of cases. This study used the volumetric software program NeuroQuant[®] (NQ) to determine specific brain structure volumes in consecutive patients (N=17) seen in a medical clinic specializing in inflammatory illness. Each of these patients presented for evaluation of an illness thought to be associated with exposure to WDB, and received an MRI that was evaluated by NQ. When compared to those of a medical control group (N=18), statistically significant differences in brain structure proportions were seen for patients in both hemispheres of two of the eleven brain regions analyzed; atrophy of the caudate nucleus and enlargement of the pallidum. In addition, the left amygdala and right forebrain were also enlarged. These volumetric abnormalities, in conjunction with concurrent abnormalities in inflammatory markers, suggest a model for structural brain injury in “mold illness” based on increased permeability of the blood brain barrier due to chronic, systemic inflammation.

1. Introduction

The awareness of acute and chronic health effects caused by exposure to the dense microbial growth found in many water-damaged buildings (WDB) has progressed steadily over the past ten years. In 2004, an expert panel from the Institute of Medicine [16] reviewed literature published through 2003, confirming that reports of respiratory effects of exposure to WDB were well supported. Later that year a consensus study from the University of Connecticut's Center for Indoor Environments and Health [53] suggested that a variety of symptoms, including headache, vertigo and memory loss, should be recorded by clinicians in suspected cases of WDB syndrome. In 2005, two clinical studies reported by our group [47,49] described a larger constellation of symptoms, including executive cognitive and neurologic symptoms, which were routinely noted in 178 affected patients but not in 111 controls. A series of laboratory findings in these patients identified innate immune inflammatory abnormalities, such as complement activation, accompanied by low levels of a critical inflammatory regulator, alpha melanocyte stimulating hormone (MSH). A prospective re-exposure trial, termed ABB`AB, performed after patients had been successfully treated for their previously persistent symptoms, showed that such symptoms, including headache and executive cognitive impairment, and laboratory abnormalities re-appeared rapidly, essentially reproducing the prior clinical status, within three days of re-exposure to WDB [47]. The observed re-acquisition of symptoms and laboratory findings in the ABB`AB trial was further reinforced by another, more intense study based on prospectively collected data. This work included a double blinded, placebo-controlled clinical trial confirming the benefits of treatment, beginning with removal from exposure and followed by the use of an orally administered anion-binding resin, cholestyramine (CSM) [46].

In 2008 the US Government Accountability Office summarized Federal research on the health effects of indoor mold [56] and in 2009, the World Health Organization report on illness acquired following exposure to damp spaces [61], both continued the expansion of the recognized role of acute and chronic inflammation in the illness. In 2010, an internally peer-reviewed consensus report from a panel of Expert Mold Treating Physicians recognized the importance of neurocognitive and neurological symptoms as well as the innate immune inflammatory basis of the illness, and termed it a chronic inflammatory response syndrome (CIRS-WDB) to describe the diversity of inflammatory problems seen in patients [48].

Although the correlation of specific serum markers is widely disputed, it is widely accepted that chronic inflammation contributes to cognitive decline, as well as neurologic disease [9]. A significant portion of case definition for CIRS-WDB relies on abnormal serum markers, important in the initiation and progression of inflammation, such as complement, TGF β 1, and the neuropeptides, vasoactive intestinal peptide (VIP) and MSH. Cognitive decline and other neurologic sequelae are persistent problems in patients with CIRS-WDB. Currently, objective assessment of central nervous system (CNS) findings in cases with neurological deficits involves magnetic resonance spectroscopy (MRS) and imaging (MRI), with estimation of brain structure swelling or atrophy mostly qualitative. Non-specific findings of gliosis and the presence of bright objects seen on T2 weighted images were found in over 45% of CIRS-WDB cases (Investigating center's unpublished data) compared to 5% in controls. Although these neurologic findings are common, no attempts to determine structural abnormalities in the CNS have ever been recorded in patients with this illness.

NeuroQuant (NQ) is a recently developed software program (CorTechs Labs, www.cortechs.net) cleared for marketing in 2006 by the US FDA for measurement of brain

structure volume from the MRI of human subjects. Since its clearance by the FDA, the reliability and validity of NQ has been supported by multiple peer-reviewed studies of normal controls and patients with Alzheimer's disease [11,12,32] other types of dementia [26], mild cognitive impairment [26,32,37] and traumatic brain injury [41,42]. Because patients with CIRS-WDB exhibit both neuropsychiatric symptoms and serum inflammatory markers known to impact blood brain barrier integrity, we used NQ in this study to determine if structural abnormalities in the brains of patients could be detected.

2. Methods

2.1 Subjects

Institutional Review Board approval for this study was granted by Copernicus Group IRB LLC, Research Triangle Park, NC. Nineteen (19) consecutive patients, between the ages of 20-60, coming to a specialized clinic for evaluation and treatment of a chronic inflammatory response syndrome, potentially acquired following exposure to the interior environment of a WDB, signed HIPAA releases to participate in a clinical trial to assess the hypothesis that their illness parameters included volumetric abnormalities in the CNS. All subjects (patients and controls) self-identified as right handed to avoid potential confounding of brain symmetry between right and left handed subjects. Each of the patients demonstrated exposure to a building with a history of water intrusion followed by evidence of microbial growth as shown by any one or more of the following: (i) presence of visible mold; (ii) presence of elevated levels of speciated fungi as shown by qPCR using ERMI (Environmental Relative Mold Index) testing; or (iii) presence of strong, musty odors. Patients were interviewed by a physician to determine the presence of symptoms consistent with CIRS [48]. Fourteen (14) patients had never been treated

and had persistent symptoms despite removal from exposure. Four (4) patients had been partially treated, including use of the bile acid sequestrant cholestyramine (a common treatment for CIRS), before their office visits but were still symptomatic. One (1) had returned to the office for a repeat bout of illness following re-exposure (relapse). Symptoms were recorded as part of a medical history; all suspected CIRS patients then underwent a specific panel of blood labs to determine current presence of proteomic abnormalities typically found in the illness.

The NeuroQuant[®] (NQ) computer-automated analysis produces volumetric data on 11 brain regions (Table 2) but only supplies control data for three of these regions. To extend our analyses, we used our own control population to assess the volumetric differences for all brain regions mapped by NQ. A group of 18 medical controls between the ages of 20-60 was recruited from a patient group coming to the clinic for well evaluation during the same time frame and (i) who had no symptoms or lab abnormalities suggesting CIRS; (ii) nor history of brain injury or executive cognitive impairment; (iii) and who had no significant uncontrolled medical illnesses.

2.2. Blood labs

Laboratory blood tests were performed by CLIA-licensed facilities, LabCorp, Quest Diagnostics, National Jewish Center (Denver) and Cambridge Biomedical. Testing included HLA DR by PCR, alpha melanocyte stimulating hormone (MSH), vasoactive intestinal peptide (VIP), leptin, matrix metalloproteinase 9 (MMP9), split product of complement component 3 (C3a) and component 4 (C4a), transforming growth factor beta-1 (TGFB1), IgG for gliadin (AGA), and IgM for cardiolipin (ACLA), vascular endothelial growth factor (VEGF), plasminogen activator inhibitor (PAI-1), cortisol, erythrocyte sedimentation rate, C reactive protein (CRP), lipid profile, complete blood count (CBC), comprehensive metabolic panel

(CMP), gamma-glutamyl transpeptidase (GGTP), thyroid stimulating hormone (TSH), lipid profile, and von Willebrand's profile. Patients were classified abnormal for von Willebrand's antigen for results either < 50 or > 150 IU. Dysregulation of simultaneously measured ACTH/cortisol and ADH/osmolality was determined by (i) absolute high (ACTH > 45 or cortisol > 21 ; ADH > 13 or osmolality > 300) or low (ACTH < 5 or cortisol < 4 ; ADH < 1.3 or osmolality < 275) values; or (ii) ACTH was below 10 when cortisol was below 7; or ADH was below 2.2 when osmolality was 292-300 for the two-paired tests; or (iii) in which ACTH was > 15 when cortisol was > 16 ; and ADH > 4.0 when osmolality was 275-278 for the two-paired tests.

The diagnosis of CIRS-WDB was made by an experienced clinician using the standard process of differential diagnosis, including assessment of exposure risks, symptoms, and blood lab results, as compared to prior cases of known CIRS-WDB and described previously [5, 17].

2.3. Brain Imaging and Analysis

Each subject in this study had (1) a magnetic resonance spectroscopy (MRS) scan measuring N-acetyl aspartate, creatinine, myoinositol and the ratio of glutamate to glutamine of lactate, (2) a magnetic resonance image (MRI) scan of the brain using 3.0 Tesla MRI scanner (Siemens) performed at Peninsula Imaging, Salisbury, Maryland, followed by (3) volumetric analysis of the image using NQ. In addition to the general requirements for having an MRI (e.g. having no magnetic metal in the head), the NQ protocol required, at a minimum, the following scan elements: (i) MRI scanning protocol based on the Alzheimer's Disease Neuroimaging Initiative (ADNI) scanning protocol; (ii) T1 timing sequence; (iii) Non-contrast; (iv) Sagittal sectioning (that is, planes of section parallel to the plane passing through the longitudinal

fissure); and (v) 3D imaging. This protocol for scanning can be found on the NQ website (<http://www.cortechslabs.net/products/neuroquant.php>).

The brain MRI data for each patient or control was uploaded to the NQ server, which processed and analyzed the brain imaging data. This computer-automated analysis involved several steps, including an active contour or “snake” model for skull stripping followed by an automated segmentation and probabilistic atlas-based methods to quantify segmental structures (details of segmentation methods can be found in [12]). The NQ program provided a full-volume spatially corrected and anatomically labeled dataset containing the absolute and relative volumes on 11 brain regions, with left and right hemispheres reported separately for each MRI scan. All mapping outputs were visually inspected for segmentation irregularities.

2.4. Statistical methods

For the current study, all data analyzed were in the normalized format of intracranial volume percentage. Statistics for brain structures were first computed across gender and then across hemispheres (in the same individuals). Further statistical comparisons were made between patients and controls of the 11 brain structures in two ways. The first used the data output from the individual hemispheres (left and right hemispheres analyzed separately) for a total of 22 comparisons (11 structures in the left hemisphere plus 11 structures in the right hemisphere), each with an N of 35 (18 controls and 17 patients). The second analysis used the same data but eliminated the distinction of hemisphere (left and right distinction dropped and each subject contributed two values for each structure) for a total of 11 structure comparisons each with an N of 70.

The 22 brain measurements generated by the software (11 brains structures in each hemisphere) for both patients and controls resulted in 44 data groups. These groups were all tested for normality using the Shapiro-Wilk test. In all of the following comparisons of volumes, both a t-test and a Kruskal-Wallis non-parametric test were calculated for each brain structure.

To assess potential differences in gender, a two-sample, two-sided t-test was performed across gender in controls and patients separately. Since natural asymmetries are known to occur between hemispheres of brain structures, asymmetry was assessed using a two-sided, paired-sample t-test on structures across hemispheres in controls and patients separately. Finally, to compare patient against control data, a two-sided, two-sample t-test with unequal variances (Welch test) was used. For purposes of statistical significance in each comparison, we applied a Holm-Bonferonni stepwise multiple test correction to an alpha of 0.05.

To determine if any correlations existed between blood lab measurements and effects on brain regions, a linear regression was performed on each pair of blood and brain variables. The Pearson correlation coefficient, r , and the p-value, p , from testing the null hypothesis $H_0: r=0$ were calculated using JMP (version 6.0.3).

3. Results

3.1. Patient demographics and diagnoses

Nineteen (19) consecutive patients reporting to a specialized clinic (The Center for Research on Biotxin Associated Illness) who met initial criteria for exposure risk and symptoms of an illness thought to be caused by exposure to a water damaged building (CIRS-WDB) were entered into the study. However, when blood labs were analyzed, two of the 19 patients did not meet all the case criteria, as discussed in Results 3.4. This left 17 cases (11 Females, 6 Males,

mean age; 41.7, std; 11.3, range; 23-56, mean yrs of education; 15.6) matched against a group of 18 medical controls (10 Females, 8 Males, mean age; 45.7, std; 8.1, range; 29-60, mean years of education; 15.3) for analysis of brain structure volume (Table S1). A diagnosis of CIRS rests heavily on key blood indicators (Table 1) and the symptoms and blood lab abnormalities in this cohort of 17 patients passed the same screening as did 1,829 other CIRS-WDB patients seen at this clinic [50]. A positive diagnosis is generally required to have 4 abnormal values out of the 9 key labs. There was a noteworthy difference in this cohort in that only 65% of the patients tested abnormal for VIP, which has historically been the best indicator of illness in patients, with abnormalities in upwards of 90% of prior cases. However, the LabCorp VIP assay has been undergoing modifications, in addition to new normative values being established. As well, historically, 61% of patients recorded abnormally high levels of MMP9, much higher than the 35% reported in this cohort. Neuropsychiatric symptoms (Figure 1) were common in patients with 100% reporting difficulties in concentrating and the ability to focus. The medical controls in this cohort did not present with symptoms of inflammatory illness and as such, the full panel of blood labs reported in cases was not prescribed. However, basic blood work for controls was unremarkable and indicated normal health status.

3.2. Volumetric analysis

When tested for normality using a Shapiro-Wilk test ($p < 0.05$), 34 of the 44 data groups were found to have normal distributions (Table S1). Non-normal control data included the Right Cortical Gray, Left Lat. Ventricle, L. Hippocampus, R. Amygdala, L. Caudate and R. Pallidum, while non-normal patient data included the L. Lat Ventricle, R. Inferior Lat Vent, L. Amygdala and R. Thalamus. Because of these non-normal groups, patient versus control comparisons also

included the Kruskal Wallis non parametric statistical test. However, to simplify presentation the non-parametric testing results are given as supplementary material (Table S1) as the parametric testing is robust enough to handle the small to moderate deviations from normality found in our data.

Because of differences in exposure loads, from different types of mycotoxins, duration of exposure and illness, as well as age, gender, diet and a myriad of other factors that can all impact disease status, a minimal amount of correlations to specific volumetric changes were attempted in this cohort. Correlations of blood lab values to changes in brain structures were not significant with only one exception. VEGF showed a mild correlation to changes in the forebrain in both hemispheres with an r of -0.58 and a p -value of 0.018. Additionally, due to small difference in age (4yrs) between controls and patients, a linear regression performed determined there were no significant differences in brain structure volumes in our study cohort due to this age difference.

Although the left and right hemispheres of the brain are largely mirror images, they are known to have a functional asymmetry, hence the terms right brain and left brain. Because the function of brain structures can show a “handedness” between left and right hemispheres, there is opportunity for greater development of a structure in one hemisphere over the other. This question had great bearing on the level of comparison for our patient to control data so our first task was to determine if detection limits using NeuroQuant (NQ) software analysis on brain MRIs could identify differences in anatomic symmetry of brain structures. For this we used a paired sample t -test and a Kruskal-Wallis test. In the control population, both tests showed that NQ identified significant variability in size between hemispheres for the hippocampus and forebrain (Table 2) in the same individuals. Patients showed a higher degree of asymmetry with four of the 11 structures, the hippocampus, forebrain, cortical gray and thalamus, exhibiting

significant differences in size between hemispheres. This makes sense if we consider that the inflammatory illness of patients could be contributing to changes in the volume of structures between hemispheres. Another, less likely scenario, is that people with brain structure asymmetry are more likely to develop CIRS. In any event, these asymmetry results revealed the importance of comparing matching sides when making assertions of abnormalities between cases versus controls, even though we present analyses of structures used without distinction of side (effectively doubling the number of data points for a structure, denoted L&R) with several significant differences (Table 3), these results are not developed further in the discussion. The comparison of structure volumes between this cohort of 18 medical controls showed no significant differences between male and female at the family-wise error rate of 0.01.

When comparing the mean values of structures between CIRS-WDB patients and controls, a generalized pattern is observed. Overall, CIRS-WDB patients showed an enlargement of parenchymal structures, coincident with a reduction in the volume of ventricles (Figure 2). The one exception to this generalization was the reduced volume of the caudate nucleus (CN). Analysis of NQ data identified statistically significant differences in normalized volume between cases of CIRS-WDB and controls in multiple brain areas. Using parametric statistics, patients exhibited a significant enlargement of the left amygdala, right forebrain and the pallidum in both hemispheres, as well as a decrease in the volume of the CN in both hemispheres. Difference in volume between patients and controls of the right hippocampus was the first structure that did not meet the level of significance using the Holm-Bonferroni stepwise multiple test correction that dictated an alpha of 0.0031 for significance while the right hippocampus produced an alpha of 0.0037 (Table 3). Even though the amygdala, pallidum and CN included at least one non-normal data set between controls and patients in either the left or right hemisphere, the non-

parametric Kruskal Wallis test also agreed with the t-test that these structures were significant ($p < 0.001$, Table S1).

3.3. *Pallidum to Caudate Nucleus ratio*

With these results in hand, we calculated a post hoc index of abnormality by using a ratio of the pallidum volume over the caudate volume (P/C) and multiplied by a constant of 100 (Figure 3). Because volumetric analyses on these structures showed significant differences in both parametric and non-parametric tests, in both hemispheres, it is not surprising that the P/C ratio also showed a statistically significant difference between patients and controls. When both hemispheres are used, the mean patient P/C ratio was 32.4 while the average control P/C was 22.7.

3.4. *Patients excluded from analysis*

Although 19 consecutive, potential CIRS-WDB cases were assigned to this study, two cases were eliminated from our analysis in the process of differential diagnosis as discussed in section 3.1. In the first case, a female presented with exposure risk and symptoms consistent with the illness, but blood labs did not pass CIRS-WDB case criteria. Although she did present with depressed levels of VIP and elevated TGFB1 of over 10,000, which are two of the best indicators of this inflammatory disorder, other lab values were inconclusive. This patient did have NQ volumetric analysis and that analysis showed a slightly elevated P/C ratio of 26.0. The second case eliminated from analysis was also a female. This patient passed all CIRS-WDB case criteria, but had an abnormal blood sugar lab of over 500 mg/dl (normal fasting blood glucose < 100 mg/dl). Because of confounding factors in this patient's illness, she was eliminated from our

overall analysis. However, this patient suffered volumetric abnormalities similar to other cases with a P/C ratio of 32.1.

4. Discussion

4.1 Summary

Although closely matched, the differences in class parameters of this study such as age, gender and sample size must be considered. Additionally, non-normal distributions in some of the datasets merit a conservative statistical approach. Having taken into consideration these facts, the findings of increases in pallidum, amygdala and forebrain volume; coupled with a decrease in volume of the caudate nucleus (CN) confirm that CNS structural changes occur in CIRS-WDB patients. Based on the analysis of 11 brain regions, 8 of the 9 parenchymal structures tended to enlarge, but only the CN parenchymal volume was reduced, possibly due to damage to the blood brain barrier caused by inflammatory markers in CIRS. The decrease in volume of the CN is likely to be due to the loss of dendritic attachments. This selective atrophy contrasts with other neurodegenerative or neuro-inflammatory conditions with volume loss from other gray matter structures [31,35,60].

4.2. Edema and Blood Brain Barrier

The blood brain barrier (BBB) is a complex partition that selectively protects the brain parenchyma by restricting passage of cells and molecules from the circulation. Composed of tight junctions between endothelial cells, adhesion and cellular matrix molecules in a basal lamina, supported by pericytes, and enveloped by astrocytes, the BBB can be injured by inflammatory stressors, including those found in CIRS patients, such as MMP9, VEGF and

TGFB1[46]. This injury can increase permeability of the BBB and may result in edema, which is well described in the literature [17,25].

An important BBB stressor is TGFB1. The wide ranging effects of this signaling molecule leave no simple explanation as to its role in BBB integrity. Working through multiple receptors, with opposing effects, the result of TGFB1 cascades on specific cell types, in specific tissues is pleiomorphic, although chronically high levels do not speak well for BBB integrity, nor most common neurological disorders (For review [7]). TGFB1 reduces tight junction adhesions in CNS derived vascular endothelium, resulting in increased paracellular permeability [44] but it can also up-regulate the tight junctions of brain vascular endothelial cells, lowering permeability [25]. Additionally, local secretion of TGFB1 by pericytes decreases permeability in capillary endothelial cells [24]. TGFB1 was elevated in over 90% of cases in a large study of CIRS-WDB patients [50] and is elevated in brains of patients with AD, MS, Parkinson's, stroke and traumatic brain injury [7]. Given so many influences, TGFB1 can be considered a master regulator, impacting the activities of many effector molecules, including MMP9 and VEGF, either directly or via multiple feedback loops.

TGFB1 was shown to quickly and durably up-regulate VEGF in vascular endothelial cells [28]. Both peripherally-derived [22] and centrally produced VEGF by astrocytes has been shown to increase vascular permeability [2] and a systemic treatment that blocked VEGF signaling improved inflammatory disease symptoms in rats [2]. VEGF can increase permeability from both the abluminal side and intra-luminally, as well as specifically increase the permeability of the BBB to compounds of small size, including a biologically produced toxin, tetanus toxin fragment C [4]. VEGF is associated with vasogenic edema in hypoxic-ischemic brain injury, as hypoxia up-regulates VEGF with a consequent increase in BBB permeability

[19]. In multiple sclerosis, astrocyte-produced VEGF drives increased BBB permeability, with the down-regulation of VEGF associated with a reduction in barrier breakdown and decreased neuropathology in mice [2,3]. In CIRS patients we see a bi-modal distribution of VEGF, with over 50% of patients outside normative values, either having elevated or reduced VEGF.

The matrix metalloproteinase MMP9, often elevated in CIRS, is associated with brain edema formation [33], with such edema further activating additional MMP9 production [10]. Disruption of the BBB from hypoxia results in increased permeability involving the rearrangement of tight junctions with disrupted continuity, gapping and increased extra-cellular matrix (ECM) destruction due to increased MMP9 [6]. Magnetic resonance spectroscopy of CIRS patients commonly reveals elevated lactate levels in the frontal lobes, which is indicative of hypoxia (data not shown). Peripheral MMP9 is not the only source of MMP9 injury to the BBB. Neuroglial-secreted MMP9 controls the composition of the extracellular matrix (ECM) that connects brain capillary endothelial cells with surrounding brain cells. Both MMP9 and VEGF increase permeability modulated by pericytes [55]. Treatment protocols for CIRS patients lower levels of MMP9, although significant increases are seen after re-exposure to the interior environment of WDB (49). MMP9 has been shown to activate all latent isoforms of TGF β [62]; in a reciprocal fashion, TGF β 1 increases MMP9 expression in astrocytes [34]. The mechanism of white matter damage following systemic inflammation is multifactorial, including cerebral inflammation and breakdown of BBBs with leakage of plasma proteins into the brain parenchyma [52]. Once initiated, increased permeability leads to extravasation of plasma proteins into white matter, which in turn induces interstitial edema, further increasing BBB permeability [59].

Low levels of the neuropeptide vasoactive intestinal peptide (VIP) and elevated complement component C4a are also common to CIRS-WDB patients. Although its importance to controlling inflammatory cascades in the periphery are well documented [30], the role of VIP on the BBB is less clear. Activation products of early components of the complement cascade (such as C4), are co-localized with beta amyloid plaques in Alzheimer's disease, but without late components [18]. This seemingly incomplete complement cascade could play a novel role in neurological illness. Taken together, the inflammatory markers seen in CIRS-WDB patients are intimately involved with BBB integrity. Having TGFB1, VEGF and MMP9 changing rapidly with exposure and re-exposure suggests that the BBB permeability will fluctuate as the inflammatory elements of CIRS-WDB change, creating the potential for ongoing fluctuations in neuropsychiatric symptoms.

4.3. Caudate nucleus has a role in executive cognitive dysfunction and neurologic disorders

The CN is an element of the basal ganglia, which also includes the putamen, globus pallidus, subthalamic nuclei and the substantia nigra. It has important frontostriatal connections that integrate neural network functioning and subserve executive cognitive functioning [38,58]. These nuclei are located at the base of the forebrain, play an important role in working memory, and are involved in fine motor and cognitive functions [31]. CN lesions lead to impairments in problem solving, mental flexibility, learning, attention, short-term and long-term memory, retrieval, and verbal fluency [58]. Caudate and thalamic nuclei play a major role in executive functioning; damage to these structures are possibly responsible for motor, cognitive, and sensory disabilities [35,38]. The CN plays a role in cognition with increasing recognition that corticostriatothalamic loops are involved in attention, executive function and movement disorder.

It also may be an important anatomical substrate of cognitive dysfunction in Parkinson's and Alzheimer's [1].

4.4 Caudate atrophy in other illnesses

The CN includes neurons and glial cells, extracellular space, dendrite proliferation and connections. Reduction of any of these components could lead to diminished volume. CN atrophy is a marker of global gray matter loss in aging and in several neurological disorders [31]. In our small cohort, the presence of caudate atrophy but not other gray matter areas is unique. There is abundant evidence for gray matter atrophy occurring in association with inflammatory illness, including rheumatoid arthritis [60], particularly in atrophy of the subcortical gray matter. A global reduction of gray matter has been described in patients with chronic pain conditions, low back pain, migraine, chronic fatigue syndrome and post-traumatic stress disorder [60]. The basal ganglia are involved in the sensory-discriminative, affective, and cognitive dimensions of pain; as well as in modulation of nociceptive information.

In multiple sclerosis, caudate atrophy is seen concomitantly with atrophy of the thalamus, globus pallidus and hippocampus. The inflammatory process is associated with atrophy of gray matter compared to white [8,45,63]. In Huntington's disease the CN is atrophic as is thalamus, midbrain, insula, and white matter [43]. Localized atrophy of a specific structure could potentially be a biomarker reflecting neuropathic processes [57].

A common misdiagnosis made in CIRS-WDB patients is fibromyalgia. Brain volumes in fibromyalgia show decreases in gray matter in the prefrontal cortex, amygdala and anterior cingulate cortex [14]. Note the increase in amygdala volume seen in the cohort reported here. Parkinson's presents a clinical entity in which caudate atrophy is present without isolated caudate atrophy [1,40].

4.5. Role of caudate in selected neuropsychiatric syndromes

Commonly seen in CIRS-WDB are a variety of neuropsychiatric symptoms, including obsessive compulsive disorder (OCD). This behavioral disorder may be due to striatal dysfunction, mainly of the CN, leading to inefficient thalamic gating, resulting in hyperactivity within the orbitofrontal cortex (intrusive thoughts) and the anterior cingulate cortex (non-specific anxiety) [23]. Other pathological behaviors triggered by the environment, such as tics in Tourette's syndrome (TS) could share similar mechanisms [13].

The inhibition of an unwanted response is an important function of the executive system. This process is impaired in patients with a dysregulated dopamine system. In such patients, Bagiayan [5] found multiple abnormalities in neurotransmission in the putamen and caudate (particularly in dorsal aspect of left caudate) during a processing task that called for executive inhibition. Poor processing performance is reported in patients with attention deficit hyperactivity disorder (ADHD), TS, Parkinson's disease, and schizophrenia, suggesting that the dopamine system of the left caudate is involved in the inhibition of unwanted responses. The suggestion is consistent with the observation of hyperactivity, agitation and inattention following lesion, destruction or shrinkage of the caudate head [15].

4.6. Glial fibrillary acidic protein, TGFB1 and caudate atrophy

The unifying mechanism for these structural brain findings is not clear. We know that the activation of astrocytes by rising TGFB1 occurs in inflammatory injury to the BBB [29], thereby resulting in release of glial fibrillary acidic protein (GFAP), which in turn results in reduced neurite outgrowth. This finding is enhanced in gray matter compared to white matter [54].

The inhibition by GFAP of neuronal regeneration is established. Mice deficient in GFAP have significantly better neuronal survival and neurite outgrowth compared to those with intact GFAP production [39]. In astrocytes, TGF β 1 was shown to activate the promoter for GFAP [21], although this activation may need a cofactor [20]. Production of GFAP is inversely linked to production of VEGF [36]. Data from studies on a BBB-disrupting spider venom [51] showed that the major areas of expression of GFAP is in gray matter.

5. Conclusions

This study demonstrates, for the first time, a distinctive CNS finding of structural, neurological injury in patients diagnosed with CIRS-WDB. The mechanisms for the observed volumetric changes are suggested to be resultant from antecedent inflammatory injury, although the theory of increased permeability of the BBB will require prospective validation. The presence of atrophy in the CN but enlargement in other areas of gray matter by itself seems a unique marker. The significant findings here could aid in identification of illness, as well as provide a basis to explore the mechanisms of neurologic abnormalities in these patients. Follow-up studies are currently underway that will leverage greater statistical power, likely expanding the significant structural abnormalities in brains of CIRS patients.

Figure Legends

Figure 1. Neuropsychiatric symptoms. Neuropsychiatric symptoms are charted as a percentage of occurrences in current patient and control cohorts (decreased assimilation of new knowledge is inability to retain read information).

Figure 2. Brain structure volumetric analysis. Volumetric analyses of brain structures in patients were normalized to control values and plotted as a percentage. Columns in red indicate statistical significance (0.0031) by parametric testing. Error bars indicate standard deviation.

Figure 3. Pallidum to caudate ratio (P/C). The pallidum to caudate ratio was plotted for current control and patient cohorts. Three measures were derived for each subject: Right pallidum/Right caudate, Left pallidum/Left caudate, and the combined Right + Left pallidum/Right + Left caudate. The mean of each cohort is represented following the individual data. * indicates statistical significance (0.005) for comparisons between case and control data for each of the three average measures.

Acknowledgements

The authors would like to thank Scott McMahon, MD and Lesley Benyon, PhD for comments and review of the manuscript.

References

- [1] O.P. Almeida, E.J. Burton, I. McKeith, A. Gholkar, D. Burn, J.T. O'Brien, MRI study of caudate nucleus volume in Parkinson's disease with and without dementia with Lewy bodies and Alzheimer's disease, *Dementia and geriatric cognitive disorders* 16 (2003) 57-63.
- [2] A.T. Argaw, L. Asp, J. Zhang, K. Navrazhina, T. Pham, J.N. Mariani, S. Mahase, D.J. Dutta, J. Seto, E.G. Kramer and others, Astrocyte-derived VEGF-A drives blood-brain barrier disruption in CNS inflammatory disease, *The Journal of clinical investigation* 122 (2012) 2454-68.
- [3] A.T. Argaw, B.T. Gurfein, Y. Zhang, A. Zameer, G.R. John, VEGF-mediated disruption of endothelial CLN-5 promotes blood-brain barrier breakdown, *Proceedings of the National Academy of Sciences of the United States of America* 106 (2009) 1977-82.
- [4] I. Ay, J.W. Francis, R.H. Brown, Jr., VEGF increases blood-brain barrier permeability to Evans blue dye and tetanus toxin fragment C but not adeno-associated virus in ALS mice, *Brain research* 1234 (2008) 198-205.
- [5] R.D. Badgaiyan, D. Wack, Evidence of dopaminergic processing of executive inhibition, *PloS one* 6 (2011) e28075.
- [6] A.T. Bauer, H.F. Burgers, T. Rabie, H.H. Marti, Matrix metalloproteinase-9 mediates hypoxia-induced vascular leakage in the brain via tight junction rearrangement, *Journal of cerebral blood flow and metabolism : official journal of the International Society of Cerebral Blood Flow and Metabolism* 30 (2010) 837-48.
- [7] K. Beck, C. Schachtrup, Vascular damage in the central nervous system: a multifaceted role for vascular-derived TGF- β , *Cell and tissue research* 347 (2012) 187-201.
- [8] N. Bergsland, D. Horakova, M.G. Dwyer, O. Dolezal, Z.K. Seidl, M. Vaneckova, J. Krasensky, E. Havrdova, R. Zivadinov, Subcortical and cortical gray matter atrophy in a large sample of patients with clinically isolated syndrome and early relapsing-remitting multiple sclerosis, *AJNR American journal of neuroradiology* 33 (2012) 1573-8.
- [9] B.M. Bettcher, J.H. Kramer, Inflammation and clinical presentation in neurodegenerative disease: a volatile relationship, *Neurocase* 19 (2012) 182-200.
- [10] T. Beziaud, X. Ru Chen, N. El Shafey, M. Frechou, F. Teng, B. Palmier, V. Beray-Berthat, M. Soustrat, I. Margaille, M. Plotkine and others, Simvastatin in traumatic brain injury: effect on brain edema mechanisms, *Critical care medicine* 39 (2011) 2300-7.
- [11] J.B. Brewer, Fully-automated volumetric MRI with normative ranges: translation to clinical practice, *Behavioural neurology* 21 (2009) 21-8.
- [12] J.B. Brewer, S. Magda, C. Airriess, M.E. Smith, Fully-automated quantification of regional brain volumes for improved detection of focal atrophy in Alzheimer disease, *AJNR American journal of neuroradiology* 30 (2009) 578-80.
- [13] A. Buot, J. Yelnik, Functional anatomy of the basal ganglia: limbic aspects, *Revue neurologique* 168 (2012) 569-75.
- [14] M. Burgmer, M. Gaubitz, C. Konrad, M. Wrenger, S. Hilgart, G. Heuft, B. Pfliegerer, Decreased gray matter volumes in the cingulo-frontal cortex and the amygdala in patients with fibromyalgia, *Psychosomatic medicine* 71 (2009) 566-73.
- [15] F.X. Castellanos, J.N. Giedd, P. Eckburg, W.L. Marsh, A.C. Vaituzis, D. Kaysen, S.D. Hamburger, J.L. Rapoport, Quantitative morphology of the caudate nucleus in attention deficit hyperactivity disorder, *The American journal of psychiatry* 151 (1994) 1791-6.

- [16] N. Clark, Ammann, H., Brennan, T., Brunekreef, B., Douwes, J., Eggleston, P., Fisk, W., Fullilove, R., Guernsey, J., Nevalainen, A., Essen, S., Damp Indoor Spaces and Health!, The National Academies Press 2004.
- [17] B.D. Cook, G. Ferrari, G. Pintucci, P. Mignatti, TGF-beta1 induces rearrangement of FLK-1-VE-cadherin-beta-catenin complex at the adherens junction through VEGF-mediated signaling, *Journal of cellular biochemistry* 105 (2008) 1367-73.
- [18] H. Crehan, J. Hardy, J. Pocock, Microglia, Alzheimer's disease, and complement, *International journal of Alzheimer's disease* 2012 (2012) 983640.
- [19] B. Davis, J. Tang, L. Zhang, D. Mu, X. Jiang, V. Biran, Z. Vexler, D.M. Ferriero, Role of vasodilator stimulated phosphoprotein in VEGF induced blood-brain barrier permeability in endothelial cell monolayers, *International journal of developmental neuroscience : the official journal of the International Society for Developmental Neuroscience* 28 (2010) 423-8.
- [20] V. De Oliveira Sousa, L. Romão, V.M. Neto, F.C.A. Gomes, Glial fibrillary acidic protein gene promoter is differently modulated by transforming growth factor-beta 1 in astrocytes from distinct brain regions, *European Journal of Neuroscience* 19 (2004) 1721-1730.
- [21] T.C. de Sampaio e Spohr, R. Martinez, E.F. da Silva, V.M. Neto, F.C. Gomes, Neuro-glia interaction effects on GFAP gene: a novel role for transforming growth factor-beta1, *The European journal of neuroscience* 16 (2002) 2059-69.
- [22] E. Dejana, C. Giampietro, Vascular endothelial-cadherin and vascular stability, *Current opinion in hematology* 19 (2012) 218-23.
- [23] A. Del Casale, G.D. Kotzalidis, C. Rapinesi, D. Serata, E. Ambrosi, A. Simonetti, M. Pompili, S. Ferracuti, R. Tatarelli, P. Girardi, Functional neuroimaging in obsessive-compulsive disorder, *Neuropsychobiology* 64 (2011) 61-85.
- [24] S. Dohgu, F. Takata, A. Yamauchi, S. Nakagawa, T. Egawa, M. Naito, T. Tsuruo, Y. Sawada, M. Niwa, Y. Kataoka, Brain pericytes contribute to the induction and up-regulation of blood-brain barrier functions through transforming growth factor-beta production, *Brain research* 1038 (2005) 208-15.
- [25] S. Dohgu, A. Yamauchi, F. Takata, M. Naito, T. Tsuruo, S. Higuchi, Y. Sawada, Y. Kataoka, Transforming growth factor-beta1 upregulates the tight junction and P-glycoprotein of brain microvascular endothelial cells, *Cellular and molecular neurobiology* 24 (2004) 491-7.
- [26] K. Engedal, A. Brækhus, O.A. Andreassen, P.H. Nakstad, Diagnosis of dementia--automatic quantification of brain structures, *Tidsskr Nor Laegeforen* 132 (2012) 1747-51.
- [27] N. Ferrara, Vascular Endothelial Growth Factor: Basic Science and Clinical Progress, *Endocrine Reviews* 25 (2004) 581-611.
- [28] G. Ferrari, G. Pintucci, G. Seghezzi, K. Hyman, A.C. Galloway, P. Mignatti, VEGF, a prosurvival factor, acts in concert with TGF-beta1 to induce endothelial cell apoptosis, *Proceedings of the National Academy of Sciences* 103 (2006) 17260-17265.
- [29] C.M. Garcia, D.C. Darland, L.J. Massingham, P.A. D'Amore, Endothelial cell-astrocyte interactions and TGF beta are required for induction of blood-neural barrier properties, *Brain research Developmental brain research* 152 (2004) 25-38.
- [30] E. Gonzalez-Rey, M. Delgado, Role of vasoactive intestinal peptide in inflammation and autoimmunity, *Current opinion in investigational drugs* 6 (2005) 1116-23.

- [31] K.M. Hasan, C. Halphen, A. Kamali, F.M. Nelson, J.S. Wolinsky, P.A. Narayana, Caudate nuclei volume, diffusion tensor metrics, and T(2) relaxation in healthy adults and relapsing-remitting multiple sclerosis patients: implications for understanding gray matter degeneration, *Journal of magnetic resonance imaging : JMRI* 29 (2009) 70-7.
- [32] D. Heister, J.B. Brewer, S. Magda, K. Blennow, L.K. McEvoy, Predicting MCI outcome with clinically available MRI and CSF biomarkers, *Neurology* 77 (2011) 1619-28.
- [33] T. Higashida, C.W. Kreipke, J.A. Rafols, C. Peng, S. Schafer, P. Schafer, J.Y. Ding, D. Dornbos, 3rd, X. Li, M. Guthikonda and others, The role of hypoxia-inducible factor-1alpha, aquaporin-4, and matrix metalloproteinase-9 in blood-brain barrier disruption and brain edema after traumatic brain injury, *Journal of neurosurgery* 114 (2011) 92-101.
- [34] H.L. Hsieh, H.H. Wang, W.B. Wu, P.J. Chu, C.M. Yang, Transforming growth factor-beta1 induces matrix metalloproteinase-9 and cell migration in astrocytes: roles of ROS-dependent ERK- and JNK-NF-kappaB pathways, *Journal of neuroinflammation* 7 (2010) 88.
- [35] R. Jech, J. Klempir, J. Vymazal, J. Zidovska, O. Klempirova, E. Ruzicka, J. Roth, Variation of selective gray and white matter atrophy in Huntington's disease, *Movement disorders : official journal of the Movement Disorder Society* 22 (2007) 1783-9.
- [36] Y.S. Kim, D.H. Jo, H. Lee, J.H. Kim, K.W. Kim, J.H. Kim, Nerve growth factor-mediated vascular endothelial growth factor expression of astrocyte in retinal vascular development, *Biochemical and biophysical research communications* 431 (2013) 740-5.
- [37] S. Kovacevic, M.S. Rafii, J.B. Brewer, I. Alzheimer's Disease Neuroimaging, High-throughput, fully automated volumetry for prediction of MMSE and CDR decline in mild cognitive impairment, *Alzheimer disease and associated disorders* 23 (2009) 139-45.
- [38] S.J. Lewis, A. Dove, T.W. Robbins, R.A. Barker, A.M. Owen, Striatal contributions to working memory: a functional magnetic resonance imaging study in humans, *The European journal of neuroscience* 19 (2004) 755-60.
- [39] V. Menet, Y.R.M. Gimenez, F. Sandillon, A. Privat, GFAP null astrocytes are a favorable substrate for neuronal survival and neurite growth, *Glia* 31 (2000) 267-72.
- [40] M. Nocker, K. Seppi, E. Donnemiller, I. Virgolini, G.K. Wenning, W. Poewe, C. Scherfler, Progression of dopamine transporter decline in patients with the Parkinson variant of multiple system atrophy: a voxel-based analysis of [123I]beta-CIT SPECT, *European journal of nuclear medicine and molecular imaging* 39 (2012) 1012-20.
- [41] D. Ross, T. Graham, A. Ochs, Review of the Evidence Supporting the Medical and Legal Use of NeuroQuant® in Patients with Traumatic Brain Injury, *Psychol Inj and Law* 6 (2013) 75-80.
- [42] D.E. Ross, C. Castelvechi, A.L. Ochs, Brain MRI volumetry in a single patient with mild traumatic brain injury, *Brain injury : [BI]* 27 (2013) 634-6.
- [43] H.H. Ruocco, L. Bonilha, L.M. Li, I. Lopes-Cendes, F. Cendes, Longitudinal analysis of regional grey matter loss in Huntington disease: effects of the length of the expanded CAG repeat, *Journal of neurology, neurosurgery, and psychiatry* 79 (2008) 130-5.
- [44] W. Shen, S. Li, S.H. Chung, L. Zhu, J. Stayt, T. Su, P.O. Couraud, I.A. Romero, B. Weksler, M.C. Gillies, Tyrosine phosphorylation of VE-cadherin and claudin-5 is associated with TGF-beta1-induced permeability of centrally derived vascular endothelium, *European journal of cell biology* 90 (2011) 323-32.

- [45] N. Shiee, P.L. Bazin, K.M. Zackowski, S.K. Farrell, D.M. Harrison, S.D. Newsome, J.N. Ratchford, B.S. Caffo, P.A. Calabresi, D.L. Pham and others, Revisiting brain atrophy and its relationship to disability in multiple sclerosis, *PloS one* 7 (2012) e37049.
- [46] R.C. Shoemaker, D.E. House, Sick building syndrome (SBS) and exposure to water-damaged buildings: time series study, clinical trial and mechanisms, *Neurotoxicology and teratology* 28 (2006) 573-88.
- [47] R.C. Shoemaker, D.E. House, A time-series study of sick building syndrome: chronic, biotoxin-associated illness from exposure to water-damaged buildings, *Neurotoxicology and teratology* 27 (2005) 29-46.
- [48] R.C. Shoemaker, Mark, L., McMahan, S., Thrasher, J., Grimes C., Research Committee Report on diagnosis and treatment of chronic inflammatory response syndrome caused by exposure to the interior environment of water-damaged buildings., in: R.C. Shoemaker (Ed.), <http://www.policyholdersofamerica.org/>, 2010.
- [49] R.C. Shoemaker, Rash, J.M., Simon, E.W., Sick Building Syndrome in water damaged buildings: generalization of the chronic biotoxin-associated illness paradigm to indoor toxigenic fungi., in: E. Johanning (Ed.), *Bioaerosols, Fungi, Bacteria, Mycotoxins and Human Health: Patho-physiology, Clinical Effects, Exposure Assessment, Prevention and Control in Indoor Environment and Work*, Saratoga Springs, NY, 2005, pp. 66-77.
- [50] R.C. Shoemaker, Ryan, J.C., Vasoactive intestinal polypeptide (VIP) corrects chronic inflammatory response syndrome (CIRS) acquired following exposure to water-damaged buildings., *Health* 5 (2013) 396-401.
- [51] L.M. Stavale, E.S. Soares, M.C. Mendonca, S.P. Irazusta, M.A. da Cruz Hofling, Temporal relationship between aquaporin-4 and glial fibrillary acidic protein in cerebellum of neonate and adult rats administered a BBB disrupting spider venom, *Toxicon : official journal of the International Society on Toxinology* 66 (2013) 37-46.
- [52] H.B. Stolp, C.J. Ek, P.A. Johansson, K.M. Dziegielewska, N. Bethge, B.J. Wheaton, A.M. Potter, N.R. Saunders, Factors involved in inflammation-induced developmental white matter damage, *Neuroscience letters* 451 (2009) 232-6.
- [53] E. Storey, Schenck, P., Dangman, K., De Bernardo, R., Yang, C., Bracker, A., and Hodgson, M., *Guidance for Clinicians on the Recognition and Management of Health Effects Related to Mold Exposure and Moisture Indoors*, University of Connecticut Health Center, Center for Indoor Environments and Health at UConn Health Center, 2004.
- [54] M. Tardy, Role of laminin bioavailability in the astroglial permissivity for neuritic outgrowth, *Anais da Academia Brasileira de Ciencias* 74 (2002) 683-90.
- [55] G. Thanabalasundaram, C. Pieper, M. Lischper, H.J. Galla, Regulation of the blood-brain barrier integrity by pericytes via matrix metalloproteinases mediated activation of vascular endothelial growth factor in vitro, *Brain research* 1347 (2010) 1-10.
- [56] USGAO, INDOOR MOLD: Better Coordination of Research on Health Effects and More Consistent Guidance Would Improve Federal Efforts United States Government Accounting Organization 2008.
- [57] S.J. van den Bogaard, E.M. Dumas, L. Ferrarini, J. Milles, M.A. van Buchem, J. van der Grond, R.A. Roos, Shape analysis of subcortical nuclei in Huntington's disease, global versus local atrophy--results from the TRACK-HD study, *Journal of the neurological sciences* 307 (2011) 60-8.

- [58] G.T. Voelbel, M.E. Bates, J.F. Buckman, G. Pandina, R.L. Hendren, Caudate nucleus volume and cognitive performance: Are they related in childhood psychopathology?, *Biological psychiatry* 60 (2006) 942-50.
- [59] K.R. Wagner, C. Dean, S. Beiler, D.W. Bryan, B.A. Packard, A.G. Smulian, M.J. Linke, G.M. de Courten-Myers, Plasma infusions into porcine cerebral white matter induce early edema, oxidative stress, pro-inflammatory cytokine gene expression and DNA fragmentation: implications for white matter injury with increased blood-brain-barrier permeability, *Current neurovascular research* 2 (2005) 149-55.
- [60] K. Wartolowska, M.G. Hough, M. Jenkinson, J. Andersson, B.P. Wordsworth, I. Tracey, Structural changes of the brain in rheumatoid arthritis, *Arthritis and rheumatism* 64 (2012) 371-9.
- [61] WHO, World Health Organization Guidelines for Indoor Air Quality: Dampness and Mould, in: E. Heseltine, Rosen, J. (Ed.), *WHO Guidelines for Indoor Air Quality: Dampness and Mould*, Geneva, 2009.
- [62] Q. Yu, I. Stamenkovic, Cell surface-localized matrix metalloproteinase-9 proteolytically activates TGF- β and promotes tumor invasion and angiogenesis, *Genes & Development* 14 (2000) 163-176.
- [63] R. Zivadinov, M. Heininen-Brown, C.V. Schirda, G.U. Poloni, N. Bergsland, C.R. Magnano, J. Durfee, C. Kennedy, E. Carl, J. Hagemeyer and others, Abnormal subcortical deep-gray matter susceptibility-weighted imaging filtered phase measurements in patients with multiple sclerosis: a case-control study, *NeuroImage* 59 (2012) 331-9.

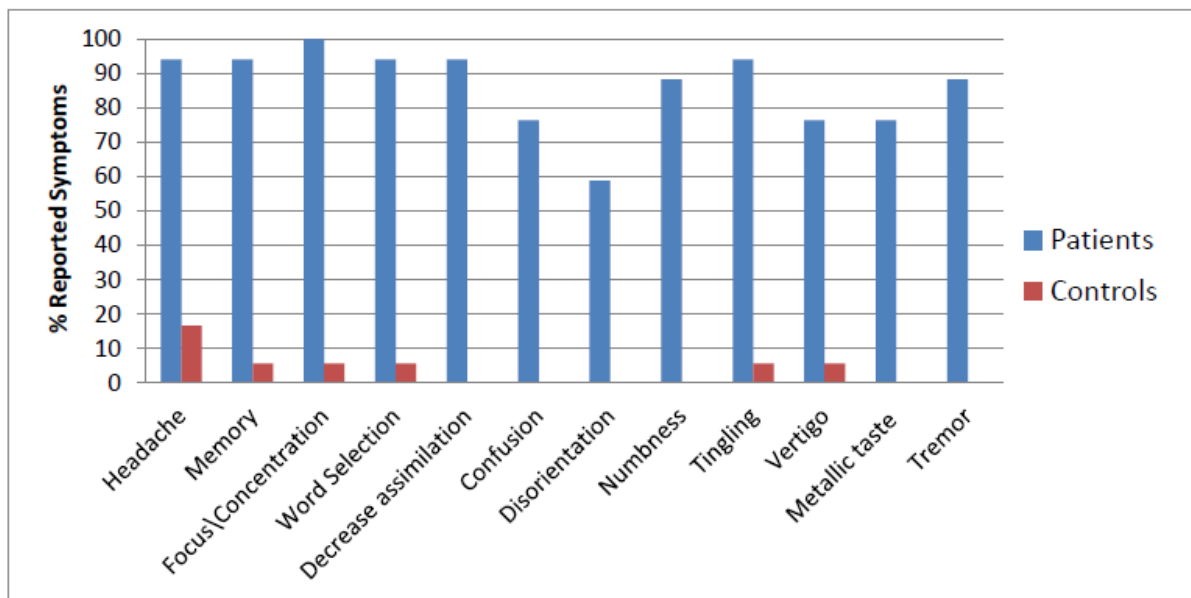


Figure 1

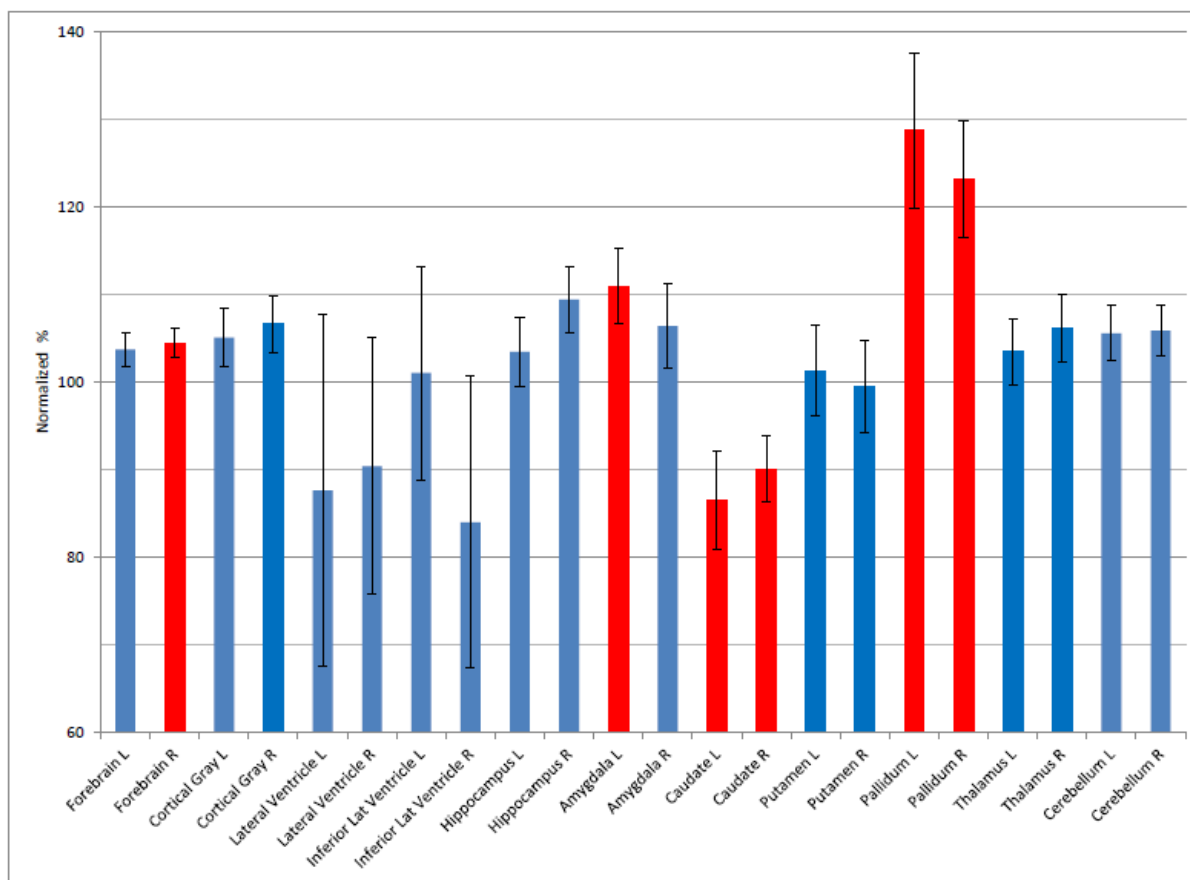


Figure 2

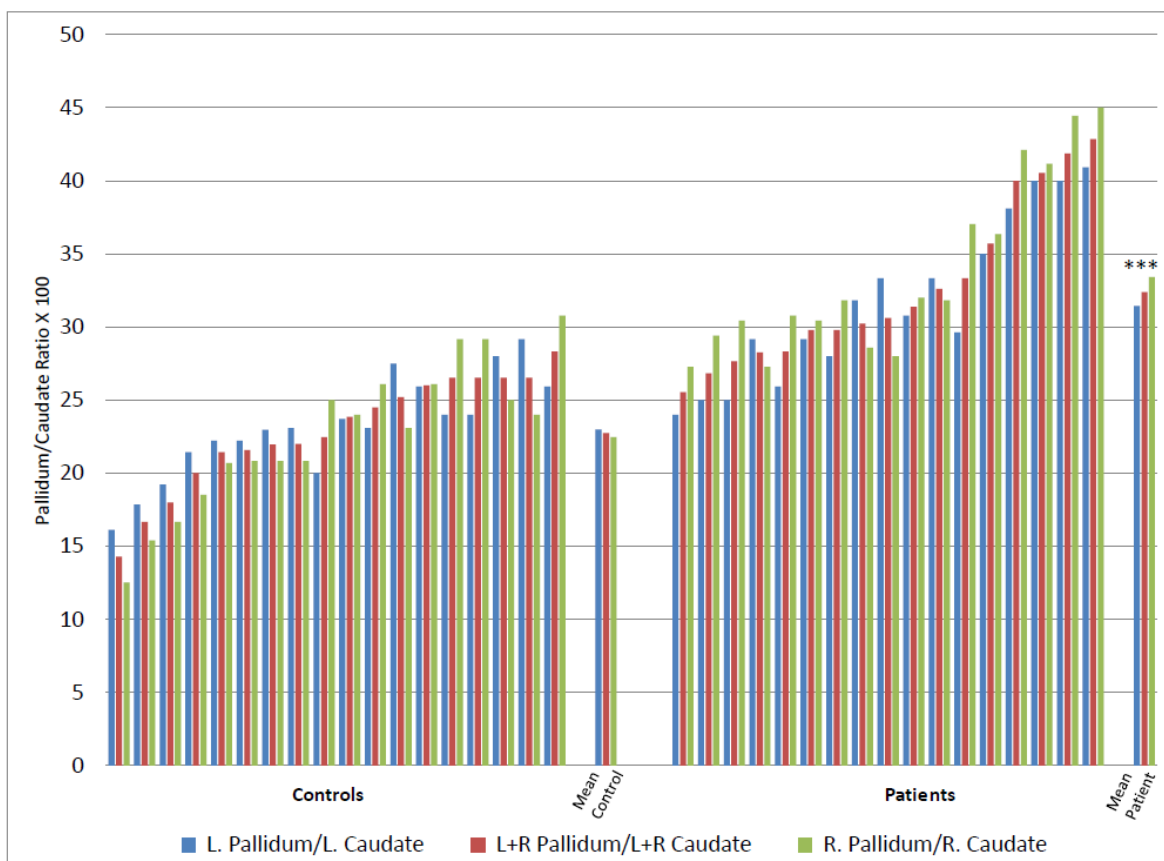


Figure 3

Table 1. Blood labs. Test value parameters of blood labs for CIRS-WDB diagnosis, the percentage of patients meeting each criterion and historical values. ADH=anti-diuretic hormone, ACTH= adrenocorticotrophic hormone

Variable	Criterion Threshold	Cases % (N=17)	Historical%
Melanocyte stimulating hormone	< 36	88%	89%
ADH/Osmolality	See Methods	88%	60%
ACTH/Cortisol	See Methods	35%	52%
Matrix metalloproteinase 9	> 330	35%	61%
Vascular endothelial growth factor	< 31 OR 86 >	59%	53%
Split product of complement 4a	> 2850	59%	72%
Transforming growth factor beta 1	> 2500	100%	88%
Vasoactive intestinal peptide	< 25	65%	91%

Table 2. Brain structure asymmetry. Mean, standard deviation (SD) and p-values of paired sample t-tests are summarized for comparisons of brain symmetry between left and right hemispheres. Statistical significance (0.0031) was determined using a Holm-Bonferroni stepwise multiple test correction. *Ho: Left Hemisphere (LH) volume = Right Hemisphere (RH) volume.

Variable	Controls (n=18)					Cases (n=17)				
	LH Mean	SD	RH Mean	SD	p-value	LH Mean	SD	RH Mean	SD	p-value
Forebrain	30.779	0.837	31.207	0.728	0.0029	31.929	1.381	32.606	1.482	<.0001
Cortical Gray	15.427	0.631	15.578	0.688	0.0089	16.211	1.488	16.609	1.439	<.0001
Lateral Ventricle	0.677	0.247	0.665	0.233	0.4694	0.593	0.255	0.601	0.142	0.8693
Inf Lat Ventricle	0.070	0.017	0.067	0.018	0.4484	0.071	0.017	0.056	0.024	0.5934
Hippocampus	0.268	0.020	0.283	0.020	<.0001	0.278	0.023	0.309	0.029	<.0001
Amygdala	0.116	0.011	0.117	0.008	0.7168	0.128	0.010	0.124	0.015	0.1101
Caudate	0.252	0.023	0.264	0.017	0.0106	0.218	0.030	0.238	0.021	0.0034
Putamen	0.347	0.033	0.341	0.028	0.2355	0.351	0.040	0.339	0.044	0.0076
Pallidum	0.057	0.011	0.061	0.007	0.0602	0.073	0.012	0.075	0.011	0.4836
Thalamus	0.508	0.033	0.524	0.029	0.0370	0.525	0.047	0.556	0.055	0.0015
Cerebellum	4.238	0.193	4.233	0.203	0.8484	4.475	0.360	4.481	0.311	0.8772

Table 3. Comparison of brain volumes between CIRS-WDB patients and medical controls. Mean, standard deviation (SD) and p-values of two-tailed t-tests are summarized. Statistical significance (0.0031) was determined using a Holm-Bonferroni stepwise multiple test correction. *Indicates data analyzed by individual hemisphere, **Indicates data analyzed without respect to hemisphere, as described in Methods.

Variable	Controls (n= 18)		Cases (n= 17)		P-value*	Controls L+R (n= 36)		Cases L+R (n= 34)		P-value**
	Mean	SD	Mean	SD		Mean	SD	Mean	SD	
Forebrain LH	30.779	0.837	31.929	1.581	0.0135	30.993	0.803	32.268	1.547	0.0001
Forebrain RH	31.207	0.728	32.606	1.482	0.0019					
Cortical Gray LH	15.427	0.651	16.211	1.488	0.0581	15.503	0.665	16.410	1.455	0.0018
Cortical Gray RH	15.578	0.688	16.609	1.439	0.0135					
Lat Ventr LH	0.677	0.247	0.593	0.255	0.3315	0.671	0.236	0.597	0.203	0.1654
Lat Ventr RH	0.665	0.233	0.601	0.142	0.3322					
Inf Lat ventr LH	0.070	0.017	0.071	0.017	0.7834	0.068	0.017	0.065	0.023	0.4466
Inf Lat ventr RH	0.067	0.018	0.056	0.024	0.1487					
Hippocampus LH	0.268	0.020	0.278	0.023	0.2070	0.276	0.021	0.294	0.030	0.0056
Hippocampus RH	0.283	0.020	0.309	0.029	0.0037					
Amygdala LH	0.116	0.011	0.128	0.010	0.0012	0.116	0.010	0.126	0.013	0.0004
Amygdala RH	0.117	0.008	0.124	0.015	0.0781					
Caudate LH	0.252	0.023	0.218	0.030	0.0007	0.258	0.021	0.228	0.027	<.0001
Caudate RH	0.264	0.017	0.238	0.021	0.0004					
Putamen LH	0.347	0.033	0.351	0.040	0.7183	0.344	0.030	0.345	0.042	0.8729
Putamen RH	0.341	0.028	0.339	0.044	0.8929					
Pallidum LH	0.057	0.011	0.073	0.012	0.0002	0.059	0.009	0.074	0.011	<.0001
Pallidum RH	0.061	0.007	0.075	0.011	0.0001					
Thalamus LH	0.508	0.033	0.525	0.047	0.2117	0.516	0.032	0.541	0.053	0.0218
Thalamu RH	0.524	0.029	0.556	0.055	0.0439					
Cerebellum LH	4.238	0.193	4.475	0.360	0.0243	4.236	0.195	4.478	0.331	0.0005
Cerebellum RH	4.233	0.203	4.481	0.311	0.0097					

Highlights

- Chronic exposure to indoor molds can cause a Chronic Inflammatory Response Syndrome (CIRS)
- CIRS, typically marked by abnormal TGFB, VIP, MMP9, VEGF, C4a and MSH can reduce BBB protection
- Patients with mold induced CIRS show significant atrophy of the caudate nucleus
- Patients with mold induced CIRS show generalized swelling of the brain parenchyma
- Patients with mold induced CIRS show generalized shrinking of brain ventricles